Title: Susceptible host availability modulates climate effects on dengue dynamics

Authors: Nicole Nova[1*], Ethan R. Deyle[2,3], Marta S. Shocket[1,4], Andrew J. MacDonald[1,5], Marissa L. Childs[6], Martin Rypdal[7], George Sugihara[2], and Erin A. Mordecai[1]

Affiliations: [1]Department of Biology, Stanford University, Stanford, CA, USA.

[2]Scripps Institution of Oceanography, University of California San Diego, La Jolla, CA, USA.

[3]Department of Biology, Boston University, Boston, MA, USA.

[4]Department of Ecology and Evolutionary Biology, University of California, Los Angeles, CA, USA.

[5]Earth Research Institute & Bren School of Environmental Science and Management, University of California Santa Barbara, Santa Barbara, CA, USA.

[6]Emmett Interdisciplinary Program in Environment and Resources, Stanford University, Stanford, CA, USA.

[7]Department of Mathematics and Statistics, UiT The Arctic University of Norway, Tromsø, Norway.

***Correspondence email:** nicole.nova@stanford.edu

Keywords: Arbovirus, climate, dengue, empirical dynamic modeling, forecasting, vector-borne disease, rainfall, susceptible population size, temperature

Abstract

Experiments and models suggest that climate affects mosquito-borne disease transmission. However, disease transmission involves complex nonlinear interactions between climate and population dynamics, which makes detecting climate drivers at the population level challenging. By analyzing incidence data, estimated susceptible population size, and climate data with methods based on nonlinear time series analysis (collectively referred to as empirical dynamic modeling), we identified drivers and their interactive effects on dengue dynamics in San Juan, Puerto Rico. Climatic forcing arose only when susceptible availability was high: temperature and rainfall had net positive and negative effects, respectively. By capturing mechanistic, nonlinear, and context-dependent effects of population susceptibility, temperature, and rainfall on dengue transmission empirically, our model improves forecast skill over recent, state-of-the-art models for dengue incidence. Together, these results provide empirical evidence that the interdependence of host population susceptibility and climate drive dengue dynamics in a nonlinear and complex, yet predictable way.

37 **INTRODUCTION**

38 Ecological systems are complex, nonlinear, and dynamic. Understanding their
39 mechanistic drivers is increasingly important in a rapidly changing world. Because
40 of this complexity, mechanistic studies are often conducted in simplified, controlled
41 environments at small scales. Connecting these experimental results with larger-
42 scale emerging patterns remains a challenge but is nonetheless imperative for
43 understanding the impacts of ecological change.

44 In concert with globalization and climate change, mosquito-borne diseases,
45 and dengue in particular, are (re)emerging globally and spreading to higher
46 latitudes (Kilpatrick & Randolph 2012; Ryan *et al.* 2019). Dengue virus—vectored
47 primarily by urban *Aedes aegypti* (Kraemer *et al.* 2015)—places half of the global
48 human population in 128 countries at risk of infection (Brady *et al.* 2012; Kraemer
49 *et al.* 2019). In the absence of effective vaccines or treatments (Katzelnick *et al.*
50 2017a; Sridhar *et al.* 2018), public health agencies rely on vector control to reduce
51 dengue transmission (Erlanger *et al.* 2008). Effective vector control interventions
52 require understanding the mechanisms linking climate, vector ecology, disease
53 transmission, and host population susceptibility to better predict disease
54 outbreaks—a major challenge.

55 Since *Aedes* spp. mosquitoes are sensitive to climate, including temperature
56 and rainfall (Stewart Ibarra *et al.* 2013; Mordecai *et al.* 2019), we expect
57 temperature and rainfall to be important drivers of dengue outbreaks. Although

58 temperature affects mosquito and viral traits in laboratory experiments (Watts *et al.*
59 1987; Lambrechts *et al.* 2011; Mordecai *et al.* 2017), the relationship between
60 temperature and dengue incidence in the field has been ambiguous (Caldwell *et al.*
61 2020). Thus, temperature-dependent models have had mixed success predicting the
62 timing and magnitudes of epidemics (Hii *et al.* 2012; Johansson *et al.* 2016; Johnson
63 *et al.* 2018). Similarly, the rainfall–dengue relationship is complex, because the
64 effect of rainfall on mosquitoes depends on local breeding habitat and human
65 behavior. In some settings, rainfall fills container-breeding habitats for mosquitoes,
66 increasing mosquito abundance and dengue incidence (Stewart Ibarra *et al.* 2013).
67 By contrast, low rainfall can also facilitate dengue transmission by promoting water
68 storage that serves as standing-water habitat for mosquitoes (Oliveira-lima *et al.*
69 2000). Further, heavy rainfall can reduce mosquito abundance by flushing out
70 larvae (Koenraadt & Harrington 2008). The net effect of climate on dengue
71 therefore depends on many different mechanisms and is highly context-dependent.

72 Disease incidence also depends nonlinearly on susceptible availability,
73 because epidemic growth slows as the population of susceptible individuals is
74 exhausted (Anderson & May 1979; Dushoff *et al.* 2004; Mina *et al.* 2015; Pitzer *et al.*
75 2015; Rypdal & Sugihara 2019). Further, susceptible availability may influence the
76 effects of climate on dengue dynamics. However, such interactive effects are difficult
77 to detect since susceptibility is difficult to observe, especially in endemic settings
78 where multiple serotypes circulate and create a complex landscape of time-
79 dependent and serotype-dependent immunity (Katzelnick *et al.* 2017b). Specifically,
80 four serotypes of dengue regularly circulate in many regions: each provides long-

term serotype-specific (homologous) immunity and short-term (heterologous) cross-protection against other serotypes (dos Santos *et al.* 2017; Jiménez-Silva *et al.* 2018; Hamel *et al.* 2019). Following a brief period of cross-protection, antibodies at a mid-range of titers can cause antibody-dependent enhancement of disease following heterologous, secondary infection, until titers decay to the point of nearly full heterologous susceptibility (Katzelnick *et al.* 2017b). Given this complex and dynamic immune landscape, directly detecting population susceptibility to circulating dengue virus at any point in time is difficult without longitudinal serology studies, which are not widely available (Gordon *et al.* 2013; Katzelnick *et al.* 2017b).

Previous prediction models of dengue outbreaks used phenomenological (Johansson *et al.* 2009b; Hii *et al.* 2012; Johnson *et al.* 2018) and mechanistic equation-based approaches (Tran *et al.* 2013; Liu-Helmersson *et al.* 2014; Morin *et al.* 2015; Mordecai *et al.* 2017), which may not fully capture interdependence between climate and susceptible availability. Phenomenological models may underperform when extrapolating past observed contexts, and equation-based mechanistic models rely on parameter estimates from laboratory studies engineered to isolate single mechanisms producing separate relationships between drivers and outcome, eliminating the complex interdependence at the population level. While laboratory studies provide robust validation of mechanisms (Lambrechts *et al.* 2011), the fixed relationships obtained from them do not necessarily translate into robust causal understanding for the complexity of field systems (Sugihara *et al.* 2012). Even if causality exists between two variables in such

104 a system, their correlation can switch signs during different time periods, resulting
105 in a net correlation of zero (Deyle *et al.* 2016b). This temporal variation in the
106 direction of correlation results from the nonlinear, state-dependent relationship
107 between the variables (i.e., the effect depends on another variable's state).
108 Conversely, even if two variables are consistently correlated, the association could
109 be spurious due to a confounder.

110 To overcome these challenges, we used empirical dynamic modeling (EDM)
111 (Sugihara *et al.* 2012)—a mechanistic, equation-free, data-driven approach that
112 accounts for the context-dependence of ecological drivers to identify and model
113 mechanisms driving dengue epidemics. EDM is based on reconstructing the
114 essential system dynamics evident in time series, without assuming fixed
115 relationships. This means relationships among variables can change through time to
116 reflect that interactions among variables depend on context and system state. EDM
117 does not require assumptions about the functional form of the model, but instead
118 derives dynamic relationships empirically by constructing an attractor—a
119 geometric object (i.e., curve or manifold) that embodies the rules for how
120 relationships among variables change with respect to each other through time
121 depending on system state (specific location on the attractor)—from time-series
122 observations. Like a set of equations, the attractor encompasses the dynamics of a
123 system, and thus can provide a mechanistic understanding of the system that is
124 derived empirically, without requiring an *a priori* assumed set of equations.

125 Here, we used EDM and a proxy for susceptible population size (Rypdal &
126 Sugihara 2019) to answer three questions: (1) Do temperature, rainfall, and/or
127 inferred susceptible availability drive population-level dengue incidence? (2) Can
128 we predict dengue dynamics using temperature and rainfall data and inferred
129 susceptible availability? (3) What is the functional form of each climate–dengue
130 relationship at the population level, and how is this relationship influenced by
131 susceptible availability?

132 **METHODS**

133 **Time series data**

134 We obtained time series of weekly observations of dengue incidence (total number
135 of new cases of all serotypes), average temperature (°C), and total rainfall (mm) in
136 San Juan, Puerto Rico, for 19 seasons (1990/1991–2008/2009) spanning calendar
137 week 18, 1990 to week 17, 2009 (Figure 1a–c) from the National Oceanic and
138 Atmospheric Administration in November 2016
139 (http://dengueforecasting.noaa.gov/). We obtained data for four additional seasons
140 (2009/2010–2012/2013) from Johnson *et al.* (2018) in April 2020
141 (https://github.com/lrjohnson0/vbdcast). Although dengue incidence data were
142 also available for Iquitos, Peru (Johansson *et al.* 2019), we chose to focus on San
143 Juan because the time series was longer, and therefore more amenable to EDM
144 analyses (Munch *et al.* 2020).

Direct measurements of susceptible availability are not available, so from weekly incidence data $I(t)$, we estimated time-dependent growth rates: $\lambda = I(t + \Delta t)/\, I(t)$. The growth rate, λ, is proportional to the effective reproduction number, R_{eff}, and equivalent to R_{eff} if Δt equals the average time between primary and secondary host infections. Vector-borne disease models show that R_{eff} is proportional to the geometric mean of the susceptible host population and the susceptible vector population: $R_{\mathrm{eff}} = \sqrt{S_{\mathrm{h}} S_{\mathrm{v}}}\, R_0$, where R_0 is the basic reproduction number (Zhao *et al.* 2020). Hence, $\lambda \propto \sqrt{S_{\mathrm{h}} S_{\mathrm{v}}}$ and λ can be used as a proxy for the susceptible population size at least during inter-outbreak periods where the transmission rate and R_0 can be assumed to vary very little (Rypdal & Sugihara 2019).

We estimated λ by linear regression using the model $I(t + \Delta t) = \lambda\, I(t)$ for 12 time points in a 12-week running window ($\Delta t = 1$ week). The model is robust to the window size (Rypdal & Sugihara 2019). In the discrete case, when $\lambda < 1$ the system is stable (inter-outbreak period) and when $\lambda \geq 1$ then the system is unstable (outbreak period) (Supporting Information). We treated the resulting time series of λ, hereafter "susceptibles index" (Figure 1d), as a proxy for the susceptible population size when $\lambda < 1$, and a proxy for the combined effects of susceptible availability and R_0 when $\lambda \geq 1$.

Empirical dynamic modeling (EDM)

EDM infers a system's mechanistic underpinnings and predicts its dynamics using time series data of one or more variables to construct an attractor in state space (Figure S1). This procedure is called univariate (using lagged versions of a single variable time series) or multivariate state-space reconstruction (SSR). Properties of the attractor are assessed to examine characteristics of the system (Deyle & Sugihara 2011). We normalized each time series to zero mean and unit variance to remove measurement unit bias, ensuring the variables would be comparable and the attractor would not be distorted. All analyses were conducted in R version 3.5.1 (R Development Core Team 2018) and all EDM analyses were performed using package `rEDM` (Park *et al.* 2020).

To infer mechanisms, EDM should be applied in systems where there is evidence of underlying low-dimensional deterministic dynamics (Cummins *et al.* 2015). EDM assumptions are met when stochasticity is present (e.g., due to measurement noise, stochastic drivers, or unexplained variability) (Cenci *et al.* 2019; Munch *et al.* 2020), but the system cannot be entirely stochastic. To test for low-dimensional deterministic dynamics we performed univariate SSR for each variable, and used *simplex projection* (Sugihara & May 1990)—a type of nearest neighbor regression performed on an attractor—to check whether the system is forecastable beyond the skill of an autoregressive model—an indicator of underlying deterministic dynamics (Figures S2a and S4; Supporting Information). To test for nonlinear state dependence of a variable—the motivation behind EDM—

186 we used the *S-map* test for nonlinearity (Sugihara 1994) (Figures S2b, c and S5;
187 Supporting Information).

188 **EDM—Convergent cross-mapping**

189 We used an EDM approach called *convergent cross-mapping* (CCM) (Sugihara *et al.*
190 2012) to identify drivers of dengue incidence. If two variables are causally related,
191 then a multivariate attractor—where each variable in the system represents a
192 dimension that traces the dynamics of the system—can be reconstructed (up to a
193 practical limit) using lagged versions of just one of the variables (Figure S1). Based
194 on Takens' Theorem, this univariate "shadow attractor" preserves the structural and
195 dynamic properties of the original multivariate attractor (Takens 1981; Sugihara *et*
196 *al.* 2012). The concept behind CCM is that if temperature causes dengue incidence,
197 then information about past temperature will be embedded in the dynamics of
198 dengue, such that the shadow attractor produced using only incidence data allows
199 us to accurately reconstruct temperature in the past. However, the converse
200 scenario would not be true: since dengue does not cause temperature, the shadow
201 attractor constructed using temperature data should not contain information to
202 accurately reconstruct past dengue incidence (Supporting Information).

203 The critical criterion for estimating causal (directional) associations between
204 two variables using CCM is checking that the cross-mapping skill (i.e., Pearson's
205 correlation coefficient, ρ, between predicted driver values using the univariate SSR
206 of the response variable, and the observed driver values) monotonically increases

and plateaus (i.e., converges) with the length of the response variable time series used in cross-mapping. We used the Kendall's τ test as a significance test for convergence of cross-mapping skill using the `Kendall` package (McLeod 2011). If $\tau > 0$ then there is convergence (Grziwotz *et al.* 2018).

We performed pairwise cross-correlations on the time series to investigate time-lagged relationships between potential drivers (i.e., temperature, rainfall, and susceptibles index) and dengue incidence using the `tseries` package (Trapletti & Hornik 2018). Based on these analyses (Figure S6), we applied a 9-week time lag between temperature and incidence, an averaged lag of 3–9 weeks for rainfall (i.e., the average rainfall over the preceding 3–9 weeks) to resemble standing water as mosquito breeding habitat over a longer time period, and a 5-week lag for the susceptibles index. These lags are proxies for the time delays of potential cause-and-effects and are consistent with results from field studies (Chen *et al.* 2010; Stewart Ibarra *et al.* 2013).

We assessed the strength of evidence for effects of potential drivers on dengue by comparing the CCM performance using the data with the performance of two null models that control for the seasonal trend (i.e., interannual mean) observed in all variables (Figure 2). These null models address the sensitivity of CCM to periodic fluctuations (i.e., seasonality), which can make two variables appear to be causally linked when instead they are simply synchronized by a seasonal confounder (Cobey & Baskerville 2016; Deyle *et al.* 2016a). In the first "seasonal" null model, we preserved the seasonal signal, but randomized the interannual

229 anomalies (Deyle *et al.* 2016a). In the second, more conservative "Ebisuzaki" null
230 model, we conserved any periodicity (beyond seasonal) and randomized the phases
231 of Fourier-transformed time series (Ebisuzaki 1997). We tested for statistically
232 significant differences in cross-mapping skill between the model that used the data
233 *versus* the null models by performing Kolmogorov-Smirnov (K-S) tests after
234 convergence.

235 We also repeated CCM in the nonsensical, reverse-causal direction (e.g., to
236 test whether incidence drives climate) as a control for potential spurious
237 relationships generated by non-causal covariation (e.g., due to seasonality). This
238 addresses the issue of synchrony, in which CCM can indicate bidirectional causality
239 when one direction is false or nonsensical (Baskerville & Cobey 2017; Sugihara *et al.*
240 2017).

241 **EDM—Forecast improvement**

242 We examined the predictive power of the drivers on dengue incidence by assessing
243 how well we can predict dengue dynamics using temperature, rainfall, susceptibles
244 index, and their combined effects. We used a combination of univariate SSR (i.e.,
245 with incidence data) and multivariate SSR to build forecasting models and to
246 determine the improvement of forecasting using simplex projection when including
247 different combinations of drivers (Dixon *et al.* 1999; Deyle *et al.* 2013, 2016a)
248 (Supporting Information). We built the SSR forecasting models/attractors using the

1990/1991–2008/2009 season data (Figure 1) and made forecasts 8 weeks ahead. We assessed model forecasting performance using leave-one-out cross-validation.

Next, we evaluated out-of-sample forecasting performance of these models using testing data from four additional seasons (2009/2010–2012/2013). Predictions made on week zero for the first forecast of the 2009/2010–2012/2013 period (8 weeks ahead) came only from SSR using the 1990/1991–2008/2009 data. All subsequent weekly forecasts (8 weeks ahead) were made from updated SSR using all previous data, including past observations from the testing dataset.

Forecast uncertainty was evaluated by taking the density and morphology of the attractor into account. The more compact a simplex was and the less its starting position on the attractor mattered for the simplex projection, the more certain we were about our point estimate. Forecast variance was obtained from a distribution of weighted nearest neighbor regression from edges of simplexes constructed at various starting positions in the past.

Finally, we compared our top model performance with performance of previous models from 16 teams that participated in a dengue forecasting challenge (Johansson *et al.* 2019) and had access to the same data. To make a fair comparison, we followed the procedure as directed in the challenge (Supporting Information).

267 **EDM—Scenario exploration**

268 In nonlinear systems, drivers generally have an effect that is state-dependent: the
269 strength and direction of the effect depends on the current state of the system.
270 Scenario exploration with multivariate EDM allowed us to assess the effect of a
271 small change in temperature or rainfall on dengue incidence, across different states
272 of the system. The outcome of these small changes allowed us to deduce the
273 relationship between each climate driver and dengue incidence and how they
274 depend on the system state. For each time step t we used S-maps (Sugihara 1994;
275 Deyle *et al.* 2016a) to predict dengue incidence using a small increase ($+\Delta X$) and a
276 small decrease ($-\Delta X$) of the observed value of driver $X(t)$ (temperature or rainfall).
277 For each putative climate driver, the difference in dengue predictions between these
278 small changes is $\Delta Y = Y(t+1)\left[X(t) + \frac{\Delta X(t)}{2}\right] - Y(t+1)\left[X(t) - \frac{\Delta X(t)}{2}\right]$, where $Y(t+$
279 $1)$ is a function of X and all other state variables, and we used $\Delta Y/\Delta X$ to approximate
280 the effect of driver X at time t. We repeated this over all time steps in our time series
281 for both temperature and rainfall to recover their approximate relationships with
282 dengue incidence at different states of the system. Scenario exploration analyses
283 were repeated across several model parameterizations to address potential
284 sensitivity to parameter settings (Supporting Information).

285 **RESULTS**

286 **Drivers of dengue dynamics**

287 EDM showed that temperature, rainfall, and the susceptibles index drive dengue
288 incidence since the convergence criterion was met (Kendall's $\tau > 0$, $P < 0.01$) in all
289 three cases (Figure 3a–c). Rainfall and susceptibles index were significant drivers of
290 dengue incidence beyond seasonality, as their effects were distinguishable from
291 seasonal and Ebisuzaki null models (Figures 3b–c and S8b–c; K-S $P < 0.0001$). This
292 implies statistically significant effects of both rainfall and the susceptibles index on
293 dengue, which are not obscured by a periodic confounder. However, temperature
294 was not a significant driver beyond seasonality (Figures 3a and S8a; K-S $P = 0.90$).
295 We cannot rule out the possibility that the apparent forcing of temperature on
296 dengue is due to a seasonal confounder. However, if no such confounder exists, then
297 the seasonal trend in temperature, which accounts for most temperature variation
298 in San Juan, drives the seasonal trend observed in dengue incidence. Compared to
299 the other drivers, the converging cross-mapping skill of the temperature null
300 models were relatively high (Figures 3 and S8), suggesting that temperature
301 seasonality in each null model was a strong driver. Thus, seasonal temperature may
302 be driving dengue dynamics, a result consistent with other studies (Huber *et al.*
303 2018; Robert *et al.* 2019).

304 As expected, EDM tests for putative causality in the nonsensical directions—
305 incidence driving temperature or rainfall—were not significant (i.e., no

306 convergence; Figure S7, black lines). This result further supports the finding that
307 temperature and rainfall drive dengue incidence, because their causal relationships
308 were not confounded by spurious bidirectionality. The null models for the
309 nonsensical directions of causality (Figure S7, grey lines) also displayed no
310 convergence (completely flat), as expected (i.e., seasonality of dengue incidence
311 does not drive seasonality of temperature or rainfall). However, seasonality (or any
312 periodicity) of temperature, rainfall and susceptibles index drive dengue dynamics,
313 shown by convergence of the seasonal and Ebisuzaki null models (grey lines in
314 Figures 3 and S8).

315 **Predictive power of drivers**

316 The multivariate SSR model using only temperature and rainfall data did not predict
317 dengue incidence very well (ρ = 0.3839, RMSE = 47.72) although it captured the
318 seasonality of the epidemics (Figure 4a). Forecasting skill doubled when the
319 susceptibles index was included along with rainfall and temperature (ρ = 0.7547,
320 RMSE = 37.40; Figure 4c), where timing and magnitude of epidemics were captured
321 reasonably well. Dengue incidence prediction improved even further when
322 incidence was added into the model with all drivers (ρ = 0.7662, RMSE = 37.14;
323 Figure 4e). Dengue incidence was somewhat predictable using univariate SSR of
324 incidence data alone (ρ = 0.4459, RMSE = 46.75; Figure 4g), suggesting that the
325 dengue incidence time series contains information about its drivers, although
326 limited. This points to some additional value of including the driver variables.

We also evaluated the performance of the SSR models (Figure 4a, c, e, g) constructed using data from seasons 1990/1991–2008/2009 on external, testing data from 2009/2010–2012/2013 that were not used in SSR (Figure 4b, d, f, h). The average out-of-sample forecasting skill for each model for the testing seasons was higher than that of the 1990/1991–2008/2009 forecasts, although the errors were larger. The model using only temperature and rainfall displayed predictability (ρ = 0.8989, RMSE = 52.30; Figure 4b), the model that also included the susceptibles index improved predictions (ρ = 0.9475, RMSE = 52.12; Figure 4d), and the model that also included past incidence made highly accurate predictions (ρ = 0.9697, RMSE = 46.75; Figure 4f). The model that only included dengue incidence without the drivers was also predictive, although more error-prone (ρ = 0.9044, RMSE = 57.34; Figure 4h). All SSR models (Figure 4a–h) had significant forecasting skill (ρ) values (Fisher's z-transformation $P < 0.001$).

The model with the highest prediction skill for the testing seasons (2009/2010–2012/2013), which included past climate, susceptibles index, and incidence data as predictors (Figure 4f), also outperformed models from the dengue forecasting challenge, including the ensemble model (Johansson *et al.* 2019) for predicting peak incidence, peak week, and seasonal incidence for all seasons on average (Tables S1–S2, Figures S9–S12). This demonstrates the benefit of the EDM approach for capturing the mechanistic, nonlinear, interdependent relationships among drivers over both equation-based mechanistic models and phenomenological models.

349 **State-dependent functional responses**

350 As expected, we find state-dependent effects of temperature and rainfall with non-
351 zero median effects. We found that temperature had a small positive median effect
352 (2.88 cases/°C, Wilcox $P < 0.001$) on dengue incidence (Figure 5a). A positive effect
353 is expected for the temperature range in Puerto Rico (Mordecai *et al.* 2017) (Figure
354 6e, black dashed lines), although the effect was occasionally much stronger, both
355 positive and negative (Figure 5a, b). The large negative effects occurred only at the
356 highest temperature values (as predicted by mechanistic models of temperature-
357 dependent transmission), reinforced by a lower quantile regression with a strongly
358 negative slope (Figure 5b, bottom dashed red line). However, positive effects
359 occurred across the whole temperature range, which is limited to temperatures
360 below the 29°C optimal temperature for transmission estimated from mathematical
361 models and laboratory data (Mordecai *et al.* 2017).

362 Rainfall had a small negative median effect (–0.12 cases/mm, Wilcox $P <$
363 0.001), but occasionally had very large negative effects (Figure 5a, c). These large,
364 negative effects of rainfall on dengue occurred when there was less than 100 mm of
365 rain per week (Figure 5c), consistent with expectations that drought could lead to a
366 high number of dengue cases due to water storage, which can provide mosquito
367 breeding habitat (Oliveira-lima *et al.* 2000). There are also small positive effects of
368 rainfall on dengue (Figure 5c), suggesting that overall the results showed competing
369 effects of low to moderate rain providing standing water for mosquito breeding and

370 humans storing water where mosquitoes can breed when there is drought or low
371 rainfall.

372 These results suggest the strength and direction of the effects of climate on
373 dengue dynamics depend on the state of the system. In addition to the nonlinear
374 effects of climate drivers themselves on dengue incidence, another potential cause
375 of state-dependent climate effects on dengue dynamics is the variation in the
376 susceptible population size over time (Figure 6a, b). Outbreaks do not occur when
377 there are too few susceptible people in the population. As expected, when the
378 susceptibles index was small ($\lambda < 0.85$) incidence was insensitive to climate (Figure
379 6c, f). By contrast, when the susceptibles index was large ($\lambda > 0.85$), temperature
380 and rainfall effects on dengue incidence appeared (Figure 6d, g). The gradual
381 increase and decrease of the rate of change of dengue as a function of temperature
382 (Figure 6d, red solid lines) aligned well with the changes in slope over the
383 increasing part (Figure 6e, black dashed lines representing the temperature range in
384 our study) of the unimodal temperature response curve for dengue transmission by
385 *Ae. aegypti* developed previously (Mordecai *et al.* 2017). This is an important
386 finding, since evidence of climate functional responses for disease dynamics is rare
387 due to the difficulty of obtaining appropriately informative field data. It is possible
388 that if we had temperature data ranging across a larger spectrum—possibly by
389 assembling data across multiple climates—that the empirical functional response
390 derived from EDM would also look unimodal. Further, when the susceptibles index
391 was high, the slope of the relationship between rainfall and dengue incidence
392 became more negative as rainfall increased, suggesting a concave-down effect of

393 rainfall on incidence (Figure 6g, h). This relationship has been difficult to
394 characterize in the field because of multiple, possibly context-dependent and lagged,
395 mechanisms linking rainfall to dengue.

396 DISCUSSION

397 High host susceptibility allows seasonal climate suitability to fuel large dengue
398 epidemics in San Juan, Puerto Rico. The effects of climate and susceptibility are
399 nonlinear, interdependent, and state-dependent, which makes inference from
400 controlled mechanistic experiments, equation-based mechanistic models, or
401 phenomenological models difficult. EDM provides an essential toolkit for identifying
402 these drivers, quantifying their predictive power, and approximating their
403 functional responses. In Puerto Rico, the causes of extensive interannual variability
404 in dengue incidence have remained a mystery, despite hypotheses that climate and
405 host susceptibility were involved. Here, we used EDM and a proxy for susceptible
406 availability to disentangle nonlinear and interactive mechanisms driving disease
407 dynamics.

408 We found that rainfall, susceptible availability, and plausibly temperature
409 (via its seasonality) interact to drive dengue incidence. Combined, these three
410 drivers predicted dengue incidence with high accuracy (Figure 4c). The EDM-based
411 forecasting model outperformed 16 models and an ensemble model in a recently
412 published dengue forecasting challenge (Johansson *et al.* 2019), suggesting that it
413 could enhance dengue control efforts if surveillance efforts continue to report

weekly case data. Finally, as expected from epidemiological theory, climate effects on dengue only appeared when susceptible availability exceeded a threshold ($\lambda > 0.85$; Figure 6).

The fact that climate effects are first observed when $\lambda \approx 0.85$ (before the onset of an outbreak, $\lambda = 1$), suggests that rainfall, and possibly temperature, have an effect on the timing of an impending epidemic. Climate could drive the transmission rate, thus influencing λ (which is proportional to both susceptible population size and R_0 when λ is close to 1), and therefore the timing of an outbreak could be attributed to the changes in transmission caused by seasonal climatic drivers (Rypdal & Sugihara 2019). The seasonality of temperature and rainfall had higher predictive skill than seasonality of susceptibles index (Figures 3 and S8, grey lines), further supporting that seasonality of incidence was associated with climate. However, the susceptibles index was critical for predicting dengue epidemic magnitudes (Figure 4c–f). Using the same data, Johnson *et al.* (2018) found that mechanistic models could predict the timing of seasonal epidemics, but that a phenomenological machine learning component was needed to capture interannual variation in epidemic magnitude. Our work suggests that the unobserved size of the susceptible population was a key missing link for predicting magnitude variation across years.

Previous studies have built models accounting for both susceptible availability and climate on dengue by reconstructing time series of susceptibles from a compartmental modeling framework (Metcalf *et al.* 2017). However, no

436 previous studies on dengue have explored the interdependence between climate
437 and susceptible population size. We showed that susceptible availability modifies
438 climate effects on dengue: climate has negligible effects unless the susceptible
439 population size is large enough (Figure 6). The interdependence of climate and
440 population susceptibility has also been studied in diseases where the opposite effect
441 was found. For example, climate effects on SARS-CoV-2 are expected to be negligible
442 when susceptible availability is high in the early stage of the emerging pandemic
443 (Baker *et al.* 2020). For influenza dynamics, population density in cities—potentially
444 a proxy for susceptible availability—also modulated climate effects on disease
445 transmission: climate effects were negligible in cities with high population densities
446 (Dalziel *et al.* 2018).

447 Because dengue susceptibility is so complex—due to the serotype dynamics
448 and time- and antibody titer-dependent cross-protection and enhancement
449 (Katzelnick *et al.* 2017b)—total population density or size may not be a reasonable
450 proxy for susceptible availability in dengue dynamics, and a direct mechanistic
451 estimate of population susceptibility will likely never be widely available for most
452 populations. Accordingly, it has been difficult for previous mechanistic models to
453 capture susceptible dynamics for dengue and their interactions with climate.
454 However, our approach provides a useful proxy that captures the susceptible
455 population dynamics even in the absence of more detailed immunological
456 information. By inferring the susceptibles index from incidence data, we were able
457 to capture the strong influence of the susceptible availability on dengue dynamics,
458 which in turn moderated the effect of climate on dengue dynamics. This result is

459 expected from theory (Kermack & McKendrick 1927; Xu *et al.* 2017), but
460 demonstrating it empirically is a unique contribution of this study.

461 Even when accounting for susceptible availability, the effects of temperature
462 and rainfall on dengue were strongly state-dependent (Figure 6d, g). This result is
463 potentially due to nonlinear effects of each climate driver (Figure 6e, h), interactions
464 and correlations between temperature and rainfall, microclimate variation over
465 space and time that is not captured by weekly averages, and complex lagged effects
466 that are not captured by a single fixed lag (e.g., 9 weeks). In Puerto Rico, mosquitoes
467 also breed in septic tanks year-round, allowing transmission to occur independently
468 from rainfall (Mackay *et al.* 2009), thus weakening the rainfall–dengue negative
469 relationship (Figure 6g). Some of this additional variation may be captured in the
470 dengue incidence time series itself, which may explain why including it improves
471 forecast skill over climate and susceptibility alone (Figure 4e, f). Despite this
472 additional variation, our results are consistent with previous studies suggesting that
473 dengue dynamics in Puerto Rico are positively associated with temperature
474 (Johansson *et al.* 2009b; Barrera *et al.* 2011; Morin *et al.* 2015), and possibly
475 negatively associated with rainfall (Johansson *et al.* 2009a; Morin *et al.* 2015), since
476 most *Ae. aegypti* pupae in Puerto Rico are produced in human-made containers
477 during periods of drought (Barrera *et al.* 2011).

478 The climate and incidence data used here have been used in multiple
479 forecasting efforts, where ensemble approaches and approaches that incorporated
480 mechanisms outperformed purely statistical approaches (Johansson *et al.* 2019).

481 However, even the high-performing forecasting methods using the same dataset,
482 and including (experimentally-derived) assumed mechanisms for the joint influence
483 of climate and susceptibility on dengue dynamics, are still error-prone to the timing
484 (on the order of weeks) and the magnitude (on the order of 50 cases) of intra-
485 annual epidemics (Morin *et al.* 2015; Johansson *et al.* 2019). Mechanisms isolated
486 independently in controlled experiments do not necessarily scale up to the
487 population level, and susceptible dynamics derived from compartmental models
488 may be too simple to properly capture true susceptibility at the population level for
489 dengue (Katzelnick *et al.* 2017b). EDM allowed us to infer mechanisms empirically
490 from population-level data, and accounted for the population-level interdependence
491 between climate and susceptible availability for forecasting, which probably
492 contributed to our model outperforming previous forecasting models and
493 ensembles (Table S1).

494 Connecting climate and dengue at the population level is challenging,
495 because causal relationships are likely to be nonlinear and state-dependent. A
496 toolkit of methods for testing hypotheses, understanding mechanisms, and making
497 predictions is essential for understanding disease dynamics in complex, natural
498 populations. Ultimately, understanding how climate-driven vector-borne diseases
499 are influenced by other variables, such as susceptible population size, is important
500 for optimizing vector control under critical conditions where climate might spark
501 epidemics. Our approach, using EDM and an inferred proxy for the susceptible
502 population size from data, confirmed that climate has nonlinear, seasonal effects on
503 dengue epidemics in San Juan, Puerto Rico, but only above a certain threshold of

504 susceptible availability. The mechanisms inferred from EDM could be applied to
505 understand and predict future ecological responses to changing environments,
506 including dengue epidemics in a world undergoing rapid environmental change.

ACKNOWLEDGEMENTS

We thank Giulio De Leo, Marcus Feldman, Dmitri Petrov, and members of the Fukami, Mordecai, Peay, and Sugihara labs for helpful feedback. NN was supported by the Bing Fellowship in Honor of Paul Ehrlich and the Stanford Data Science Scholars program. ERD and GS were supported by the National Science Foundation (NSF) DEB-1655203, NSF-ABI-1667584, DoD-Strategic Environmental Research and Development Program (SERDP) 15 RC-2509; Lenfest Foundation Award 00028335 and the McQuown Chair in Natural Sciences, University of California, San Diego. MSS and EAM were supported by an NSF Ecology and Evolution of Infectious Diseases grant (DEB-1518681). EAM was also supported by an NSF Rapid Response Research grant (RAPID 1640780), an NIH NIGMS R35 MIRA award (R35GM133439), the Stanford University Woods Institute for the Environment Environmental Ventures Program, the Hellman Faculty Fellowship, a Stanford King Center Seed Grant, and the Terman Fellowship. AJM was supported by an NSF Postdoctoral Research Fellowship in Biology (1611767). MLC was supported by the Lindsay Family E-IPER Fellowship and Illich-Sadowsky Interdisciplinary Graduate Fellowship.

523 **REFERENCES**

524 Anderson, R.M. & May, R.M. (1979). Population biology of infectious diseases: Part I.
525 *Nature,* 280, 361–367.

526 Baker, R.E., Yang, W., Vecchi, G.A., Metcalf, C.J.E. & Grenfell, B.T. (2020). Susceptible
527 supply limits the role of climate in the early SARS-CoV-2 pandemic. *Science*,
528 369, 315–319.

529 Barrera, R., Amador, M. & MacKay, A.J. (2011). Population dynamics of *Aedes*
530 *aegypti*and dengue as influenced by weather and human behavior in san juan,
531 puerto rico. *PLoS Negl. Trop. Dis.*, 5, e1378.

532 Baskerville, E.B. & Cobey, S. (2017). Does influenza drive absolute humidity? *Proc.*
533 *Natl. Acad. Sci.*, 114, 201700369.

534 Brady, O.J., Gething, P.W., Bhatt, S., Messina, J.P., Brownstein, J.S., Hoen, A.G., *et al.*
535 (2012). Refining the Global Spatial Limits of Dengue Virus Transmission by
536 Evidence-Based Consensus. *PLoS Negl. Trop. Dis.*, 6, e1760.

537 Caldwell, J., LaBeaud, D., Lambin, E., Stewart-Ibarra, A., Ndenga, B., Mutuku, F., *et al.*
538 (2020). Climate explains geographic and temporal variation in mosquito-borne
539 disease dynamics on two continents. *bioRxiv*, 2020.02.07.938720.

540 Cenci, S., Sugihara, G. & Saavedra, S. (2019). Regularized S-map for inference and
541 forecasting with noisy ecological time series. *Methods Ecol. Evol.*, 2041–
542 210X.13150.

543 Chen, S.C., Liao, C.M., Chio, C.P., Chou, H.H., You, S.H. & Cheng, Y.H. (2010). Lagged

temperature effect with mosquito transmission potential explains dengue variability in southern Taiwan: Insights from a statistical analysis. *Sci. Total Environ.*, 408, 4069–4075.

Cobey, S. & Baskerville, E.B. (2016). Limits to causal inference with state-space reconstruction for infectious disease. *PLoS One*, 11, 1–22.

Cummins, B., Gedeon, T. & Spendlove, K. (2015). On the Efficacy of State Space Reconstruction Methods in Determining Causality. *SIAM J. Appl. Dyn. Syst.*, 14, 335–381.

Dalziel, B.D., Kissler, S., Gog, J.R., Viboud, C., Bjørnstad, O.N., Metcalf, C.J.E., *et al.* (2018). Urbanization and humidity shape the intensity of influenza epidemics in U.S. cities. *Science*, 362, 75–79.

Deyle, E.R., Fogarty, M., Hsieh, C., Kaufman, L., Maccall, A.D. & Munch, S.B. (2013). Predicting climate effects on Pacific sardine. *Proc. Natl. Acad. Sci. U. S. A.*, 110, 6430–6435.

Deyle, E.R., Maher, M.C., Hernandez, R.D., Basu, S. & Sugihara, G. (2016a). Global environmental drivers of influenza. *Proc. Natl. Acad. Sci.*, 113, 13081–13086.

Deyle, E.R., May, R.M., Munch, S.B. & Sugihara, G. (2016b). Tracking and forecasting ecosystem interactions in real time. *Proc. R. Soc. B Biol. Sci.*, 283.

Deyle, E.R. & Sugihara, G. (2011). Generalized theorems for nonlinear state space reconstruction. *PLoS One*, 6.

Dixon, P.A., Milicich, M.J. & Sugihara, G. (1999). Episodic fluctuations in larval supply. *Science*, 283, 1528–1530.

566 Dushoff, J., Plotkin, J.B., Levin, S.A. & Earn, D.J.D. (2004). Dynamical resonance can
567 account for seasonality of influenza epidemics. *Proc. Natl. Acad. Sci. U. S. A.*, 101,
568 16915–16916.

569 Ebisuzaki, W. (1997). A method to estimate the statistical significance of a
570 correlation when the data are serially correlated. *J. Clim.*, 10, 2147–2153.

571 Erlanger, T.E., Keiser, J. & Utzinger, J. (2008). Effect of dengue vector control
572 interventions on entomological parameters in developing countries: A
573 systematic review and meta-analysis. *Med. Vet. Entomol.*

574 Gordon, A., Kuan, G., Mercado, J.C., Gresh, L., Avilés, W., Balmaseda, A., *et al.* (2013).
575 The Nicaraguan Pediatric Dengue Cohort Study: Incidence of Inapparent and
576 Symptomatic Dengue Virus Infections, 2004-2010. *PLoS Negl. Trop. Dis.*, 7,
577 e2462.

578 Grziwotz, F., Strauß, J.F., Hsieh, C. & Telschow, A. (2018). Empirical Dynamic
579 Modelling Identifies different Responses of *Aedes Polynesiensis* Subpopulations
580 to Natural Environmental Variables. *Sci. Rep.*, 8, 16768.

581 Hamel, R., Surasombatpattana, P., Wichit, S., Dauvé, A., Donato, C., Pompon, J., *et al.*
582 (2019). Phylogenetic analysis revealed the co-circulation of four dengue virus
583 serotypes in Southern Thailand. *PLoS One*, 14, e0221179.

584 Hii, Y.L., Zhu, H., Ng, N., Ng, L.C. & Rocklöv, J. (2012). Forecast of Dengue Incidence
585 Using Temperature and Rainfall. *PLoS Negl. Trop. Dis.*, 6, e1908.

586 Huber, J.H., Childs, M.L., Caldwell, J.M. & Mordecai, E.A. (2018). Seasonal
587 temperature variation influences climate suitability for dengue, chikungunya,

588 and Zika transmission. *PLoS Negl. Trop. Dis.*, 12, e0006451.

589 Jiménez-Silva, C.L., Carreño, M.F., Ortiz-Baez, A.S., Rey, L.A., Villabona-Arenas, C.J. &
590 Ocazionez, R.E. (2018). Evolutionary history and spatio-temporal dynamics of
591 dengue virus serotypes in an endemic region of Colombia. *PLoS One*, 13,
592 e0203090.

593 Johansson, M.A., Apfeldorf, K.M., Dobson, S., Devita, J., Buczak, A.L., Baugher, B., *et al.*
594 (2019). An open challenge to advance probabilistic forecasting for dengue
595 epidemics. *Proc. Natl. Acad. Sci.*, 116, 24268–24274.

596 Johansson, M.A., Cummings, D.A.T. & Glass, G.E. (2009a). Multiyear climate
597 variability and dengue - El Niño southern oscillation, weather, and dengue
598 incidence in Puerto Rico, Mexico, and Thailand: A longitudinal data analysis.
599 *PLoS Med.*, 6, e1000168.

600 Johansson, M.A., Dominici, F. & Glass, G.E. (2009b). Local and global effects of climate
601 on dengue transmission in Puerto Rico. *PLoS Negl. Trop. Dis.*, 3, e382.

602 Johansson, M.A., Reich, N.G., Hota, A., Brownstein, J.S. & Santillana, M. (2016).
603 Evaluating the performance of infectious disease forecasts: A comparison of
604 climate-driven and seasonal dengue forecasts for Mexico. *Sci. Rep.*, 6, 33707.

605 Johnson, L.R., Gramacy, R.B., Cohen, J., Mordecai, E., Murdock, C., Rohr, J., *et al.*
606 (2018). Phenomenological forecasting of disease incidence using
607 heteroskedastic gaussian processes: A dengue case study. *Ann. Appl. Stat.*, 12,
608 27–66.

609 Katzelnick, L.C., Coloma, J. & Harris, E. (2017a). Dengue: knowledge gaps, unmet

needs, and research priorities. *Lancet Infect. Dis.*, 17, e88–e100.

Katzelnick, L.C., Gresh, L., Halloran, M.E., Mercado, J.C., Kuan, G., Gordon, A., *et al.* (2017b). Antibody-dependent enhancement of severe dengue disease in humans. *Science*, 358, 929–932.

Kermack, W.O. & McKendrick, A.G. (1927). A Contribution to the Mathematical Theory of Epidemics. *Proc. R. Soc. A Math. Phys. Eng. Sci.*, 115, 700–721.

Kilpatrick, A.M. & Randolph, S.E. (2012). Drivers, dynamics, and control of emerging vector-borne zoonotic diseases. *Lancet*.

Koenraadt, C.J.M. & Harrington, L.C. (2008). Flushing effect of rain on container-inhabiting mosquitoes *Aedes aegypti* and *Culex pipiens* (Diptera: *Culicidae*). *J. Med. Entomol.*, 45, 28–35.

Kraemer, M.U.G., Reiner, R.C., Brady, O.J., Messina, J.P., Gilbert, M., Pigott, D.M., *et al.* (2019). Past and future spread of the arbovirus vectors *Aedes aegypti* and *Aedes albopictus*. *Nat. Microbiol.*, 4, 854–863.

Kraemer, M.U.G., Sinka, M.E., Duda, K.A., Mylne, A.Q.N., Shearer, F.M., Barker, C.M., *et al.* (2015). The global distribution of the arbovirus vectors *Aedes aegypti* and *Ae. Albopictus*. *Elife*, 4.

Lambrechts, L., Paaijmans, K.P., Fansiri, T., Carrington, L.B., Kramer, L.D., Thomas, M.B., *et al.* (2011). Impact of daily temperature fluctuations on dengue virus transmission by *Aedes aegypti*. *Proc. Natl. Acad. Sci. U. S. A.*, 108, 1–6.

Liu-Helmersson, J., Stenlund, H., Wilder-Smith, A. & Rocklöv, J. (2014). Vectorial capacity of *Aedes aegypti*: Effects of temperature and implications for global

632 dengue epidemic potential. *PLoS One*, 9.

633 Mackay, A.J., Amador, M., Diaz, A., Smith, J. & Barrera, R. (2009). Dynamics of *Aedes*
634 *aegypti* and *Culex quinquefasciatus* in Septic Tanks. *J. Am. Mosq. Control Assoc.*,
635 25, 409–416.

636 McLeod, A.I. (2011). Kendall: Kendall rank correlation and Mann-Kendall trend test.

637 Metcalf, C.J.E., Walter, K.S., Wesolowski, A., Buckee, C.O., Shevliakova, E., Tatem, A.J.,
638 *et al.* (2017). Identifying climate drivers of infectious disease dynamics: Recent
639 advances and challenges ahead. *Proc. R. Soc. B Biol. Sci.*

640 Mina, M.J., Metcalf, C.J.E., De Swart, R.L., Osterhaus, A.D.M.E. & Grenfell, B.T. (2015).
641 Long-term measles-induced immunomodulation increases overall childhood
642 infectious disease mortality. *Science*, 348, 694–699.

643 Mordecai, E.A., Caldwell, J.M., Grossman, M.K., Lippi, C.A., Johnson, L.R., Neira, M., *et*
644 *al.* (2019). Thermal biology of mosquito-borne disease. *Ecol. Lett.*, ele.13335.

645 Mordecai, E.A., Cohen, J.M., Evans, M. V., Gudapati, P., Johnson, L.R., Lippi, C.A., *et al.*
646 (2017). Detecting the impact of temperature on transmission of Zika, dengue,
647 and chikungunya using mechanistic models. *PLoS Negl. Trop. Dis.*, 11,
648 e0005568.

649 Morin, C.W., Monaghan, A.J., Hayden, M.H., Barrera, R. & Ernst, K. (2015).
650 Meteorologically driven simulations of dengue epidemics in San Juan, PR. *PLoS*
651 *Negl. Trop. Dis.*, 9, e0004002.

652 Munch, S.B., Brias, A., Sugihara, G. & Rogers, T.L. (2020). Frequently asked questions
653 about nonlinear dynamics and empirical dynamic modelling. *ICES J. Mar. Sci.*,

654 77, 1463–1479.

655 Oliveira-lima, W., Hodgson, J.C., Pontes, R.J.S. & Freeman, J. (2000). Vector densities
656 that potentiate dengue outbreaks in a Brazilian city. *Trop. Med.*, 62, 378–383.

657 Park, J., Smith, C., Sugihara, G. & Deyle, E.R. (2020). rEDM: Empirical Dynamic
658 Modeling ('EDM'). R package version 1.6.1.

659 Pitzer, V.E., Viboud, C., Alonso, W.J., Wilcox, T., Metcalf, C.J., Steiner, C.A., *et al.* (2015).
660 Environmental Drivers of the Spatiotemporal Dynamics of Respiratory
661 Syncytial Virus in the United States. *PLoS Pathog.*, 11, 1–14.

662 Robert, M.A., Christofferson, R.C., Weber, P.D. & Wearing, H.J. (2019). Temperature
663 impacts on dengue emergence in the United States: Investigating the role of
664 seasonality and climate change. *Epidemics*, 28.

665 Ryan, S.J., Carlson, C.J., Mordecai, E.A. & Johnson, L.R. (2019). Global expansion and
666 redistribution of *Aedes*-borne virus transmission risk with climate change. *PLoS*
667 *Negl. Trop. Dis.*, 13, e0007213.

668 Rypdal, M. & Sugihara, G. (2019). Inter-outbreak stability reflects the size of the
669 susceptible pool and forecasts magnitudes of seasonal epidemics. *Nat.*
670 *Commun.*, 10, 2374.

671 dos Santos, T.P., Cruz, O.G., da Silva, K.A.B., de Castro, M.G., de Brito, A.F., Maspero,
672 R.C., *et al.* (2017). Dengue serotype circulation in natural populations of *Aedes*
673 *aegypti*. *Acta Trop.*, 176, 140–143.

674 Sridhar, S., Luedtke, A., Langevin, E., Zhu, M., Bonaparte, M., Machabert, T., *et al.*
675 (2018). Effect of Dengue Serostatus on Dengue Vaccine Safety and Efficacy. *N.*

Engl. J. Med., 379, 327–340.

Stewart Ibarra, A.M., Ryan, S.J., Beltrá N, E., Mejía, R.L., Silva, M. & Muñ Oz, N. (2013). Dengue Vector Dynamics (*Aedes aegypti*) Influenced by Climate and Social Factors in Ecuador: Implications for Targeted Control. *PLoS One*, 8.

Sugihara, G. (1994). Nonlinear forecasting for the classification of natural time series. *Philos. Trans. R. Soc. A Math. Phys. Eng. Sci.*, 348, 477–495.

Sugihara, G., Deyle, E.R. & Ye, H. (2017). Reply to Baskerville and Cobey: Misconceptions about causation with synchrony and seasonal drivers. *Proc. Natl. Acad. Sci.*, 114, 201700998.

Sugihara, G., May, R., Ye, H., Hsieh, C., Deyle, E., Fogarty, M., *et al.* (2012). Detecting Causality in Complex Ecosystems. *Science*, 338, 496–500.

Sugihara, G. & May, R.M. (1990). Nonlinear forecasting as a way of distinguishing chaos from measurement error in time series. *Nature,* 344, 734–741.

Takens, F. (1981). Detecting strange attractors in turbulence. In: *Dynamical Systems and Turbulence, Warwick 1980, Lecture Notes in Mathematics* (eds. Rand, D. & Young, L.-S.). Springer, Berlin, Heidelberg., pp. 366–381.

Tran, A., L'Ambert, G., Lacour, G., Benoît, R., Demarchi, M., Cros, M., *et al.* (2013). A rainfall- and temperature-driven abundance model for *Aedes albopictus* populations. *Int. J. Environ. Res. Public Health*, 10, 1698–1719.

Trapletti, A. & Hornik, K. (2018). tseries: Time Series Analysis and Computational Finance.

697 Watts, D.M., Burke, D.S., Harrison, B.A., Whitmire, R.E. & Nisalak, A. (1987). Effect of
698 temperature on the vector efficiency of *Aedes aegypti* for dengue 2 virus. *Am. J.*
699 *Trop. Med. Hyg.*, 36, 143–152.

700 Xu, L., Stige, L.C., Chan, K.-S., Zhou, J., Yang, J., Sang, S., *et al.* (2017). Climate variation
701 drives dengue dynamics. *Proc. Natl. Acad. Sci.*, 114, 113–118.

702 Zhao, S., Musa, S.S., Hebert, J.T., Cao, P., Ran, J., Meng, J., *et al.* (2020). Modelling the
703 effective reproduction number of vector-borne diseases: The yellow fever
704 outbreak in Luanda, Angola 2015-2016 as an example. *PeerJ*, 2020.

705

FIGURES

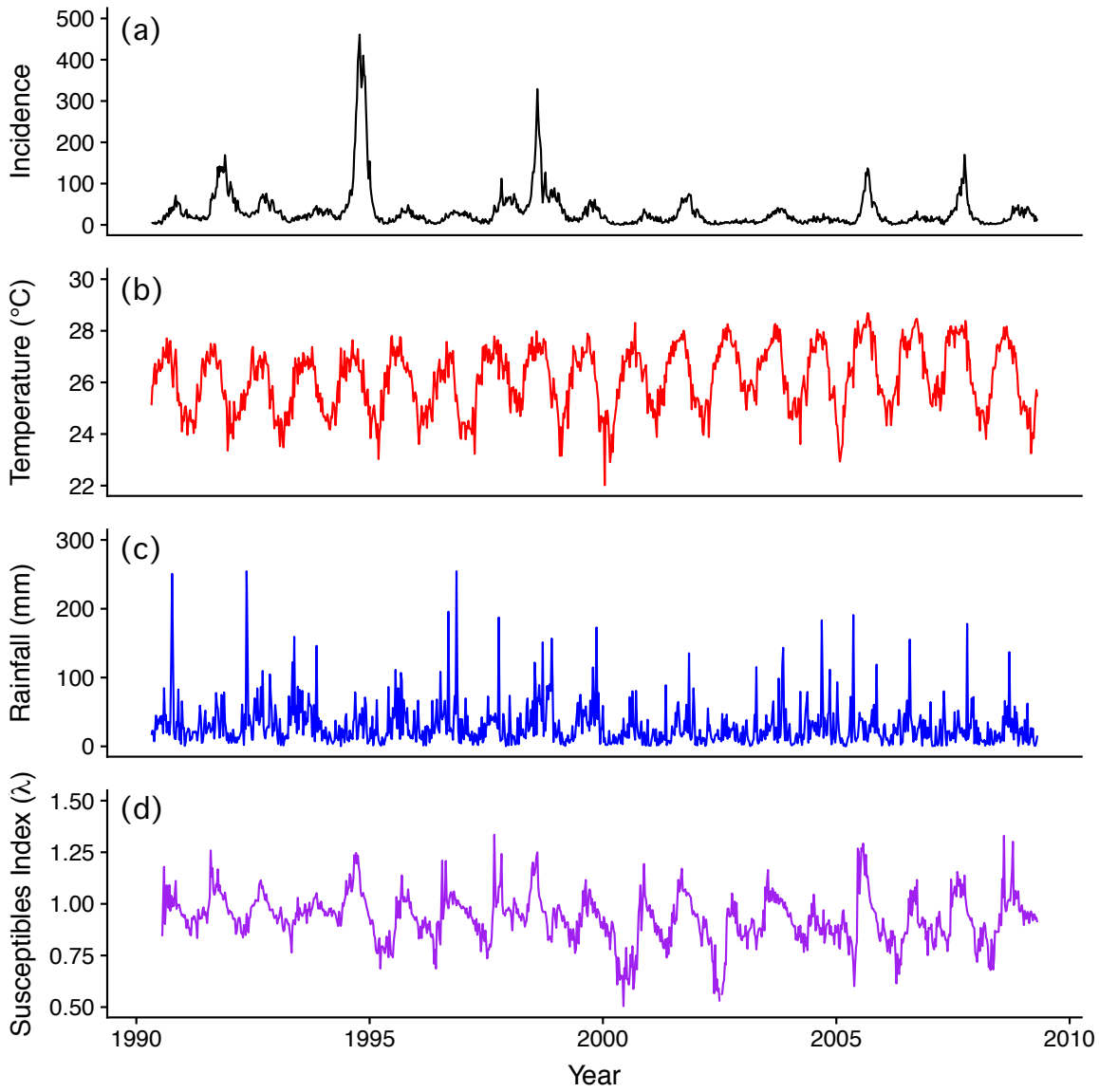

Figure 1. Dengue incidence, climate, and susceptibles index data. Time series (seasons 1990/1991–2008/2009) of (a) weekly dengue incidence (i.e., total number of cases per week), (b) weekly average temperature, (c) total weekly rainfall, and (d) a proxy for susceptible population size (see Supporting Information for details) in San Juan, Puerto Rico.

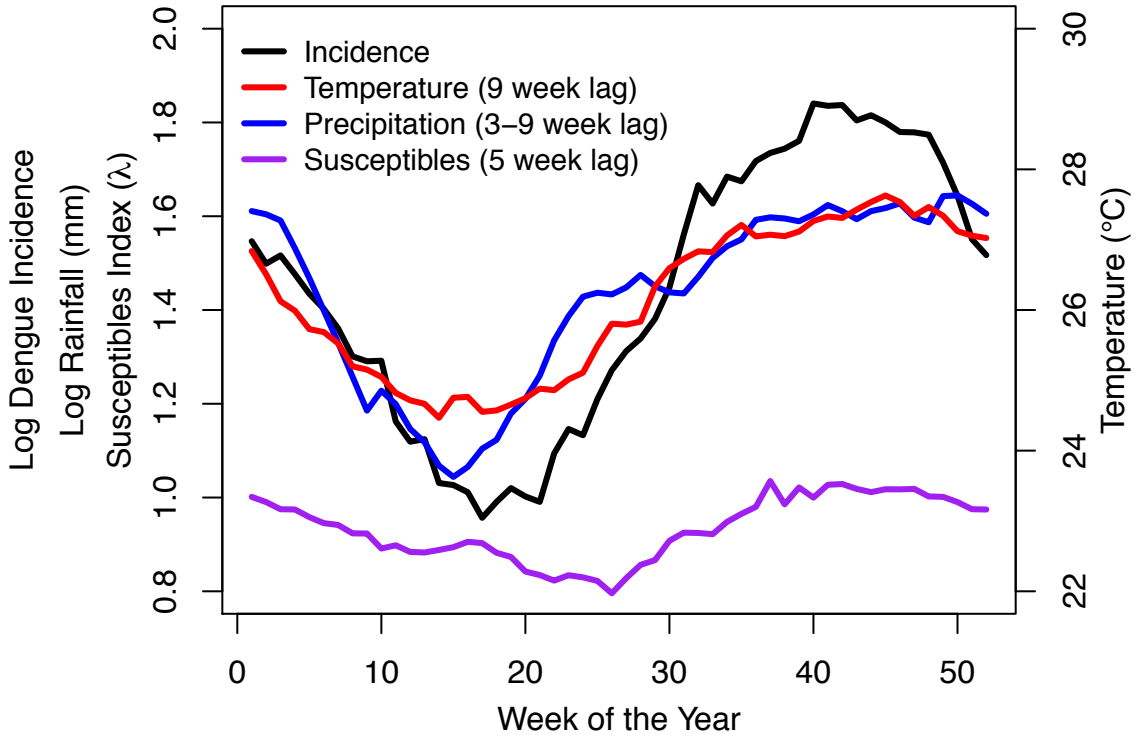

713

714 **Figure 2. Seasonal trends and lags of dengue incidence and its drivers.** The
715 strong seasonal signal of dengue cases and other variables suggests potential causal
716 lags between dengue incidence and temperature, rainfall, or the proxy for the
717 susceptible population size. The lines represent interannual averages for each week
718 of the year (i.e., calendar week) of dengue incidence (black), temperature shifted 9
719 weeks forward in time (red), average rainfall over the preceding 3–9 weeks and
720 shifted 3 weeks forward in time (blue), and susceptibles index shifted 5 weeks
721 forward in time (purple).

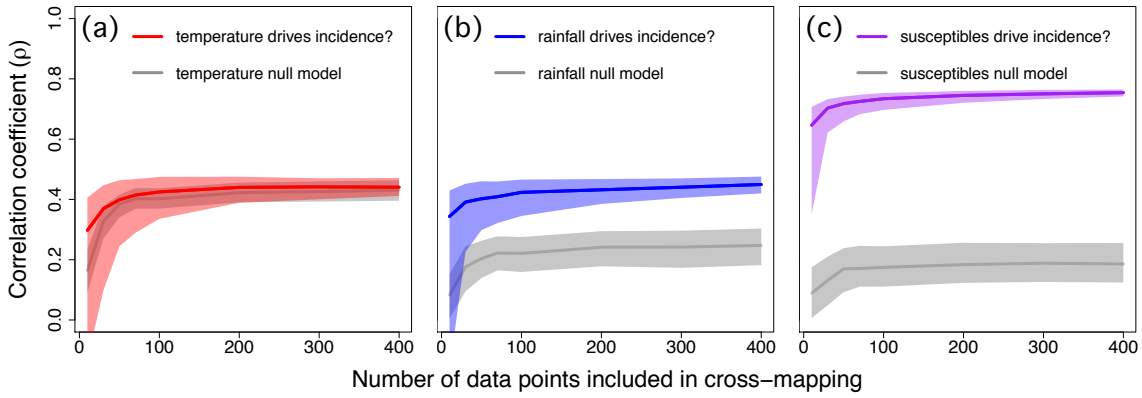

Figure 3. Climate and susceptibles index drive dengue incidence. Cross-mapping between dengue incidence and temperature (a; red), rainfall (b; blue), or susceptibles index (c; purple) display significant (Kendall's $\tau > 0$; $P < 0.01$) convergence in cross-mapping skill (i.e., ρ increases and reaches an asymptote) as the length of the time series increases (a signal of putative causality). Red, blue and purple shaded regions represent the 0.025 and 0.975 quantiles of bootstrapped time series segments. Grey shaded regions represent the 0.025 and 0.975 quantiles of the seasonal null distributions obtained from 500 runs of randomized time series with conserved seasonal trends (Deyle *et al.* 2016a). Solid lines represent medians of distributions. Rainfall and susceptibles index showed significant forcing above and beyond seasonal signal (K-S $P < 0.0001$), because cross-mapping of the true time series (blue and purple) are distinguishable from their respective null models (grey), whereas temperature forcing was not distinguishable from the null (K-S $P = 0.90$).

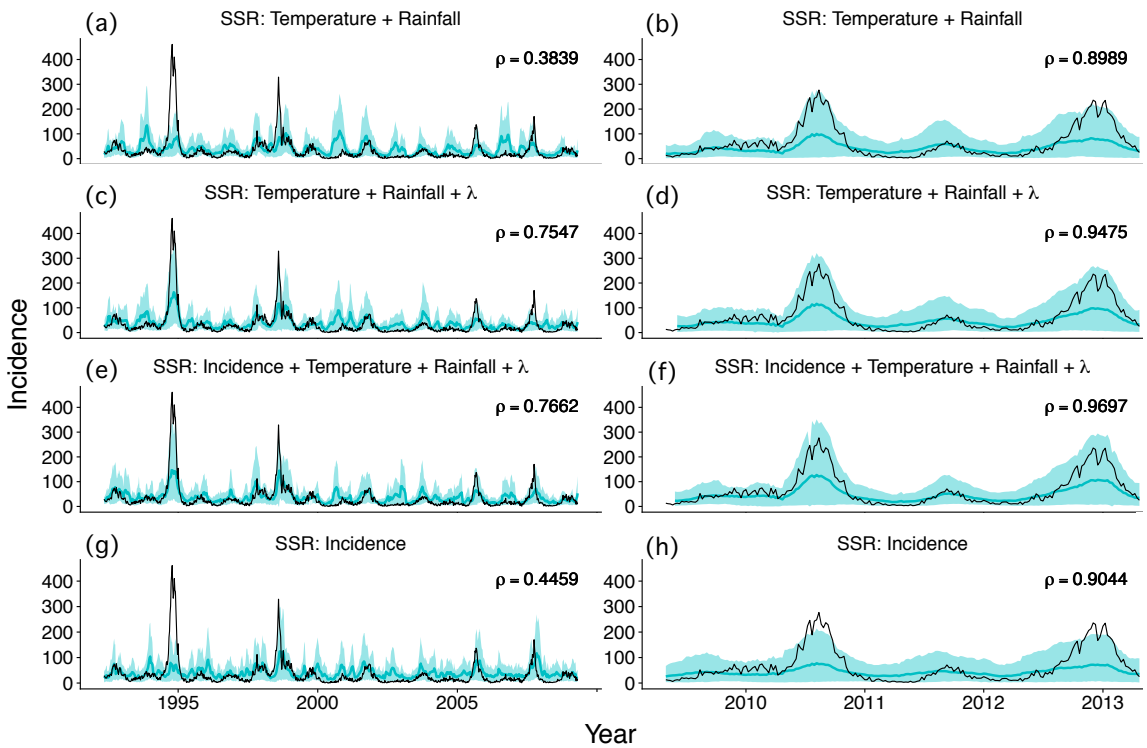

Figure 4. Predictive power of climate and susceptibles index (λ) on in-sample (left) and out-of-sample (right) dengue incidence. Forecasting results of incidence (8 weeks ahead) are shown in turquoise (solid lines represent the mean; shaded regions represent 90% confidence intervals) and observed incidence in black. (a, c, e, g) Time series for seasons 1990/1991–2008/2009 were used to construct SSR models for forecasts using leave-one-out cross-validation. (b, d, f, h) Data for seasons 2009/2010–2012/2013 were used to evaluate the SSR models constructed in a, c, e, and g, respectively, for out-of-sample forecasts. All SSR models (a–h) had significant forecasting skill (ρ) values (Fisher's z-transformation $P <$ 0.001).

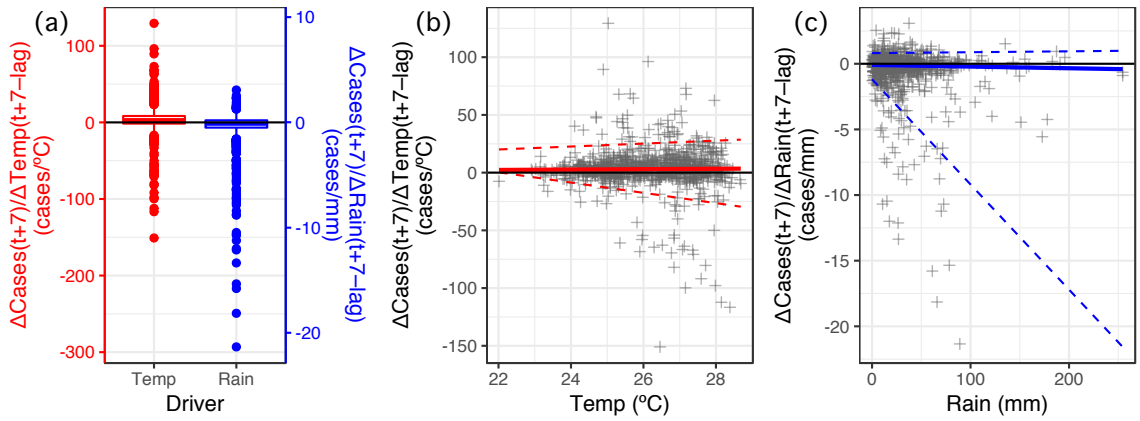

Figure 5. Temperature and rainfall show mixed effects on dengue incidence. Scenario exploration quantified the variable effect of changes in drivers on dengue. Boxplots show that the median effects of rainfall (Rain) and temperature (Temp) are small (close to zero), but drivers occasionally have strong impacts (a). To investigate climate driver functional responses, we plotted the rate of change of dengue incidence as a function of temperature (b) and rainfall (c). Red and blue lines represent regression on the median for temperature and rainfall, respectively, in a quantile regression. The dashed red and blue lines represent regression on the 0.05 and 0.95 quantiles of temperature and rainfall, respectively. Temperature has an overall positive effect on dengue incidence (median regression line of the rate of change is positive), but can also have large negative and positive effects (a, b). Rainfall has an overall negative effect (median regression line of the rate of change is negative), but can also have small positive and large negative effects (a, c).

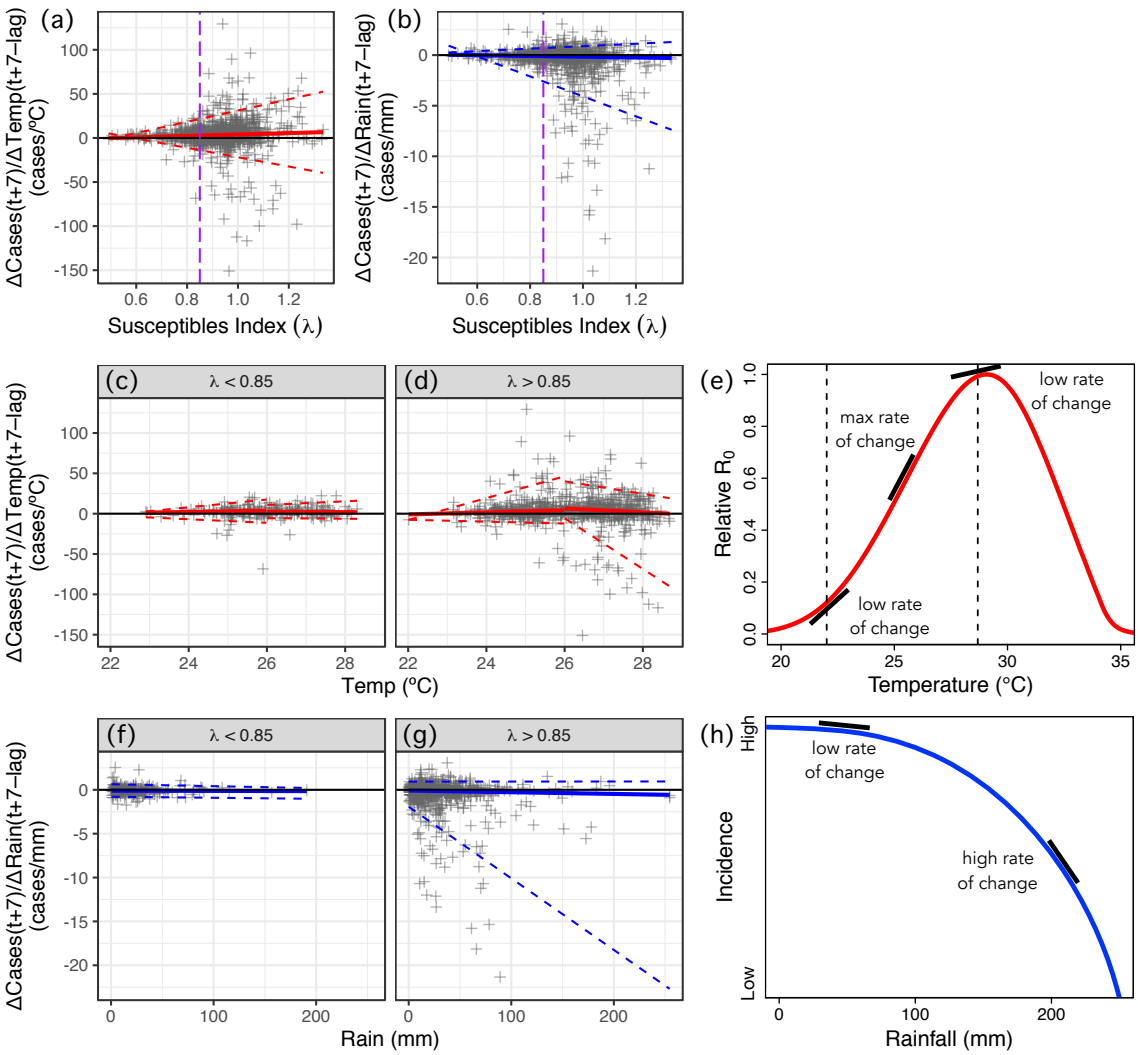

Figure 6. Temperature and rainfall effects on dengue incidence vary depending on the susceptible population size (λ). The effect of changes in temperature (a) and rainfall (b) against λ shows that driver effects are split around the threshold $\lambda \approx 0.85$ (purple dashed line). The red and blue lines represent the median regression of temperature and rainfall effects, respectively, in a quantile regression (a–d, f, g). The dashed red and blue lines represent the 0.05 and 0.95 quantile regressions of temperature and rainfall effects, respectively (a–d, f, g). Neither driver has an effect on dengue incidence when susceptible availability is low

($\lambda < 0.85$; c, f). However, when $\lambda > 0.85$ climate effects are observed: temperature has mostly a positive effect (d), possibly sigmoidal in that temperature range (e), and rainfall has a negative effect (g), and conceptually a concave down functional response (h; black lines represent tangents, where the slope of the tangent is the rate of change). The effect of temperature on relative R_0 of dengue assuming transmission via *Aedes aegypti* mosquitoes is unimodal (Mordecai *et al.* 2017) over a large temperature range (e; dashed lines indicate the minimum and maximum temperature values in the data of our study, black lines represent tangents, where the slope of the tangent is the rate of change of relative R_0 of dengue as a function of temperature). Assuming that relative R_0 is proportional to dengue incidence, our results suggest that the rate of change of dengue incidence is increasing until reaching a maximum and then decreasing (d; red median regression lines). However, even when driver effects are split at the evident threshold of $\lambda = 0.85$ (c, d, f, g), there are still many occurrences when the susceptible population size is sufficient large ($\lambda > 0.85$) but temperature and rainfall have no effect. In certain cases, temperature has even a negative effect on dengue (d).